

Gabor Wavelet Correlogram Algorithm for Image Indexing and Retrieval

H. Abrishami Moghaddam
K. N. Toosi University of Technology,
Tehran, Iran
moghadam@saba.kntu.ac.ir

M. Saadatmand-Tarzjan
K. N. Toosi University of Technology,
Tehran, Iran
saadatmand@kiaeee.org

Abstract

In this paper, a new algorithm called Gabor wavelet correlogram (GWC) is proposed for image indexing and retrieval. GWC is an effort to extend our former wavelet correlogram algorithm by introducing rotation invariant features using Gabor wavelets. We also present some ideas in order to handle effectively the redundancy problem due to non-orthogonal decomposition of Gabor wavelets. Additionally, we use an optimized weighted relative distance measure to improve the retrieval performance. The retrieval results obtained by applying GWC to a 1000 image database demonstrated significant improvements in rank, precision, and recall compared to the wavelet correlogram and enhanced wavelet correlogram algorithms.

1. Introduction

Content-based image indexing retrieval (CBIR) becomes a real demand for storage and retrieval of images in digital image libraries and other multimedia databases. In such systems, some features are extracted from every picture and stored as an index vector. In retrieval phase, every index is compared (using a distance measure) to find some similar pictures to the query image [1]. Two major approaches including spatial and transform domain based methods can be identified in CBIR systems. The first approach usually uses pixel (or a group of adjacent pixels) features like color, texture, and shape. Color histogram [2], image partitioning [3], histogram refinement [4], and color correlogram [5] are examples of the spatial domain indexing retrieval algorithms.

In the second approach, transformed data are used to extract some higher level features. Recently, wavelet based methods which provide better local spatial information in transform domain have been used [6-10]. In [6], the histograms of Daubechies wavelet coefficients in three scales were processed to construct index vectors. In SIMPLICITY [7], the image was first

classified into different semantic classes using a kind of texture classification algorithm. Then, Daubechies wavelets were used to extract feature vectors. Another approach called wavelet correlogram [8-9] used the correlogram of high frequency wavelet coefficients to construct the index. In later works [10-11], the authors presented an enhanced version of the wavelet correlogram method (EWC) using optimal quantization thresholds.

In this paper, we present Gabor wavelet correlogram (GWC) which is an effort for improving the rotation invariance property of the wavelet correlogram algorithm. We also present effective methods to address the redundancy problem caused by non-orthogonal decomposition of Gabor wavelets. Finally, in order to improve the algorithm performance, we use an evolutionary-optimized distance measure in the retrieval phase.

This paper is organized as follows: the wavelet correlogram method is reviewed in Section 2. Section 3 explains the proposed indexing retrieval algorithm. Experimental results are given in Section 4. Finally, Section 5 is devoted to concluding remarks.

2. Wavelet Correlogram

Wavelet correlogram applies the color correlogram method [5] to the wavelet coefficients of an image. Therefore, it inherits the multiscale multiresolution properties from wavelet transform and translation invariance property from color correlogram.

2.1. Wavelet correlogram indexing algorithm

Wavelet correlogram indexing algorithm consists of three steps [8-9]. First, the discrete wavelet transform of the input image is computed in three consecutive scales using Daubechies wavelets. Then, the wavelet coefficients are quantized into four levels. Finally, horizontal and vertical autocorrelograms of quantized coefficients are computed for LH and HL submatrices in each scale, respectively.

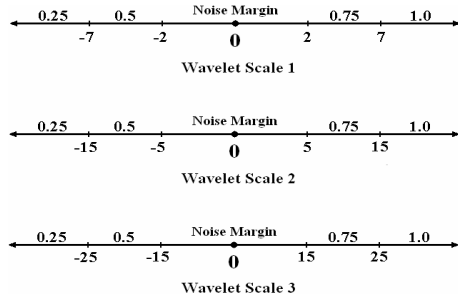


Figure 1. Wavelet correlogram quantization thresholds.

Quantization process discretizes the wavelet coefficients into four levels according to their scale. Quantization thresholds corresponding to each wavelet scale are illustrated in Fig. 1. As shown, small coefficients around zero are considered as noise and discarded. Horizontal autocorrelogram of discretized LH coefficients with distances $k \in \{1,2,3,4\}$ is defined as follows: $\alpha(i,k) = \frac{\sum_{j=1}^N \sum_{l=1}^N \left[\left(\left| \left\{ \begin{matrix} LH(x,y) = c_i; LH(x,y+k) = c_i \text{ or } LH(x,y-k) = c_i \end{matrix} \right\} \right| \right) \right]}{2 \times \left[\left| \left\{ (x,y) \mid LH(x,y) = c_i \right\} \right|}$ (1)

where c_i -s are quantization levels. Indeed, $\alpha(i,k)$ is the probability of finding two pixels with quantization level c_i at the same row of LH in a distance $k \in \{1,2,3,4\}$ of each other. Vertical autocorrelogram is applied to HL coefficients in the same manner.

The wavelet correlogram index vector is simply constructed by using autocorrelogram coefficients computed for LH and HL wavelet matrices in each scale. Each matrix gives 16 coefficients resulting in a total of 96 words per index [8].

2.2. Wavelet correlogram retrieval algorithm

In the retrieval phase of wavelet correlogram, after computing the index of the input image, all the database images are sorted according to L_1 distance measure [9]. Then, N images with the minimum distances are retrieved and shown to the user.

3. Proposed approach

Wavelet correlogram was originally developed using Daubechies wavelets for their regularity and compactness [8]. Since these wavelets are only computed in horizontal and vertical directions, the wavelet correlogram suffers from rotation variancy of the index vector. In order to overcome this problem, we propose the use of Gabor wavelet transform. Although in [9] some directions for using Gabor wavelets were given by the authors, the whole algorithm was not practically implemented.

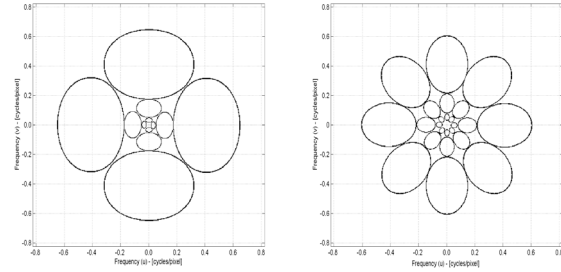


Figure 2. Two illustrations of the real-valued even symmetric Gabor filters in the frequency domain.

3.1. Construction of the Gabor wavelets

A 2D Gabor function is a Gaussian modulated by a complex sinusoid [12]:

$$\psi(x,y) = \frac{1}{2\pi\sigma_x\sigma_y} \exp\left[-\frac{1}{2}\left(\frac{x^2}{\sigma_x^2} + \frac{y^2}{\sigma_y^2}\right) + 2\pi j ax\right] \quad (2)$$

The Gabor wavelets are obtained by dilation and rotation of the generating function $\psi(x,y)$ as follows:

$$\psi_{m,n}(x,y) = a^{-m} \psi\left[a^{-m}(x \cos \theta + y \sin \theta), a^{-m}(x \sin \theta + y \cos \theta)\right] \quad (3)$$

where, $\theta = n\pi/K$; $m \in \{0, \dots, S-1\}$ and $n \in \{0, \dots, K-1\}$ represent scale and orientation, respectively; and K and S are the number of desired orientations and scales, respectively. Equation (2) can be written in the frequency domain as follows:

$$\psi(x,y) = \frac{1}{2\pi\sigma_u\sigma_v} \exp\left[-\frac{1}{2}\left(\frac{(u-\omega)^2}{\sigma_u^2} + \frac{v^2}{\sigma_v^2}\right)\right] \quad (4)$$

where, $\sigma_u = 1/2\pi\sigma_x$ and $\sigma_v = 1/2\pi\sigma_y$. Gabor functions do not result in an orthogonal decomposition, which means that a wavelet transform based upon the Gabor wavelet is redundant [12]. Manjunath and Ma [13] proposed a design strategy to project the filters so as to ensure that the half-peak magnitude supports of the filter responses in the frequency spectrum touch one another. By doing this, it can be ensured that the filters will capture the maximum information with minimum redundancy. Hence, the parameters a , σ_u , and σ_v are computed by (5)-(7), respectively:

$$a = (U_h/U_l)^{(1/S-1)} \quad (5)$$

$$\sigma_u = \frac{(a-1)U_h}{(a+1)\sqrt{2 \ln 2}} \quad (6)$$

$$\sigma_v = \tan\left(\frac{\pi}{2K}\right) \left[U_h - \left(\frac{\sigma_u^2}{U_h}\right) 2 \ln 2 \right] / \sqrt{2 \ln 2 - \frac{(2 \ln 2)^2 \sigma_u^2}{U_h^2}} \quad (7)$$

where, U_l and U_h are the upper and lower bound of the designing frequency band, respectively. The resulted real-valued even symmetric Gabor filters, which are oriented over a range of 180° , are more appropriate for image indexing purposes [13]. Examples of such Gabor filters in the frequency domain are shown in Fig. 2.

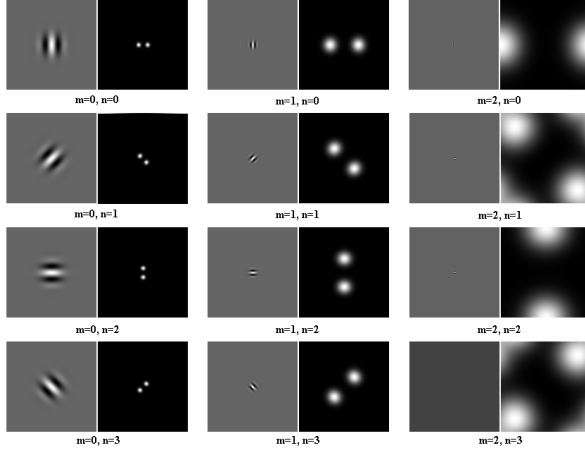


Figure 3. Illustrations of the used Gabor wavelets in the spatial (left images) and frequency (right images) domain.

3.2. Proposed indexing algorithm

We used Gabor wavelets in four directions ($K=4$) and three scales ($S=3$) as illustrated in Fig. 3. The parameters U_l and U_h are experimentally chosen as 0.05 and 0.49, respectively.

The block diagram of GWC is shown on Fig. 4. According to this figure, GWC computes first the wavelet coefficients using Gabor wavelets. The next block whose task is reducing the data redundancy will be explained in the following subsection. Then, the coefficients are discretized using the quantization thresholds obtained experimentally for good performance (Fig. 5). As illustrated in Fig. 5, small coefficients are considered as noise (and discarded) and the negative coefficients are truncated to suppress the undesirable effects of sinusoid oscillations of the Gabor wavelets. Finally, the autocorrelogram of the quantized coefficients is computed along the direction normal to Gabor wavelet orientation:

$$\alpha_{m,n}(i,k) = \frac{\left\{ \begin{array}{l} W_{m,n}(x'_0, y'_0) = c_i; \\ (x, y) \left\{ \begin{array}{l} W_{m,n}(x'_k, y'_k) = c_i \text{ or } W_{m,n}(x'_{-k_m}, y'_{-k_m}) = c_i \end{array} \right. \end{array} \right\}}{2 \times \left\{ (x, y) \left\{ \begin{array}{l} W_{m,n}(x, y) = c_i \end{array} \right. \right\}} \quad (8)$$

where, $W_{m,n}$ is the matrix of the quantized wavelet coefficients computed by $\psi_{m,n}$, k_m indicates the distance parameter of autocorrelogram and x'_k and y'_k are given by:

$$\begin{bmatrix} x'_k \\ y'_k \end{bmatrix}^T = \begin{bmatrix} \sin \theta & \cos \theta \\ -\cos \theta & \sin \theta \end{bmatrix} \begin{bmatrix} x' \\ y' \end{bmatrix} + \begin{bmatrix} k \sin \theta \\ k \cos \theta \end{bmatrix} \quad (9)$$

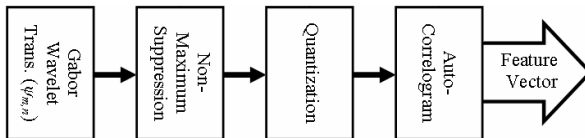


Figure 4. Block diagram of GWC.

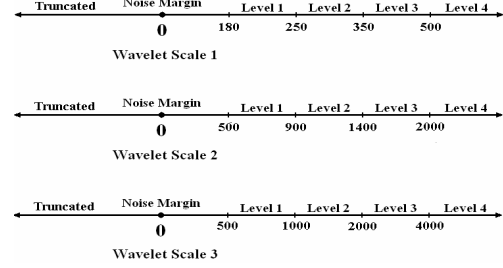


Figure 5. GWC quantization thresholds.

The index vector of GWC simply consists of the autocorrelogram coefficients computed for all Gabor wavelets including $16 \times 4 \times 3 = 192$ words.

3.2.1. Handling the redundancy problem

Gabor wavelet coefficients are redundant because of non-orthogonal decomposition. The redundant coefficients may abnormally increase the value of the correlogram coefficients. To overcome this problem, we suppress non-maximum wavelet coefficients along the wavelet orientation. Furthermore, the redundancy along the direction perpendicular to the wavelet direction is avoided by adapting the distance parameter k_m in (8) according to the wavelet scale as follows:

$$k_m \in \{2^m \times \alpha \mid \alpha = 1, 3, 5, 7\} \quad (10)$$

In more details, each 2^m adjacent wavelet coefficients are significantly dependent in m -th wavelet scale due to the redundancy. These dependent coefficients are ignored by choosing the distance parameter of autocorrelogram as multiples of 2^m .

3.3 Proposed retrieval algorithm

GWC retrieval algorithm is similar to wavelet correlogram except that it uses evolutionary optimized weighted relative distance measure (d_1) instead of L_1 [10]. It was experimentally found that d_1 provides better performance for wavelet correlogram based methods.

4. Results and discussion

We applied GWC to a subset of COREL database [7] with 1000 images in 10 categories as listed in Table 1. Fig. 6 illustrates two query results using GWC. A retrieved image has been considered a match if it belongs to the same category of the query image. The GWC is compared with wavelet correlogram [9] and EWC [10] in terms of average rank, precision, and recall. Rank (C), precision (P), and recall (R) for query image I_k ($k=1, \dots, 1000$) are defined as:

$$C(I_k) = \sum_{I_i \in A(I_k)} Rank(I_i) / |A(I_k)| \quad (11)$$

$$P(I_k, N) = \left\{ \left| \{ I_i | Rank(I_i) < N, i = 1, \dots, 1000 \} \right| / N \right\} \quad (12)$$

$$R(I_k) = P(I_k, |A(I_k)|) \quad (13)$$

Table 1. Results of GWC compared to wavelet correlogram and EWC.

Category	Wavelet Correlogram			EWC			GWC		
	\bar{C}	$\bar{P}(N=10)\%$	$\bar{R}\%$	\bar{C}	$\bar{P}(N=10)\%$	$\bar{R}\%$	\bar{C}	$\bar{P}(N=10)\%$	$\bar{R}\%$
1 Africans	288.4	55.9	29.5	283.0	57.5	31.1	263.9	52.9	33.2
2 Beaches	340.8	50.0	28.9	335.5	49.5	28.7	357.7	42.0	26.2
3 Buildings	315.8	48.3	29.3	308.6	50.6	30.5	332.8	47.8	26.5
4 Buses	112.7	86.4	62.7	109.2	87.0	63.9	111.6	88.3	65.1
5 Dinosaurs	420.7	74.0	26.2	410.5	74.8	28.8	135.3	96.2	65.0
6 Elephants	241.0	54.3	30.9	236.2	55.4	30.4	242.6	65.9	37.0
7 Flowers	150.3	81.4	58.6	126.4	84.2	65.1	194.4	75.5	50.4
8 Horses	266.9	75.7	36.7	264.9	78.4	40.0	269.3	73.0	39.5
9 Mountains	334.7	42.6	23.0	325.3	46.6	25.0	372.4	35.2	20.1
10 Food	242.3	54.5	34.7	236.8	57.2	36.5	192.7	63.2	43.1
Total	271.4	62.3	36.1	263.6	64.1	38.0	247.3	64.1	40.6

where, $A(I_k)$ represents the set of all matched images with I_k and $|A(I_k)|$ gives the number of its members. The average rank for images belonging to the q -th category (A_q) has been computed by:

$$\bar{c}_q = \sum_{k \in A_q} C(I_k) / |A_q|, \quad q = 1, 2, \dots, 10 \quad (14)$$

Finally, the total average rank is given by:

$$\bar{C} = \sum_{q=1}^{10} \bar{c}_q / 10 \quad (15)$$

The average precision and recall are also computed in the same manner. As shown in Table 1, the proposed algorithm performed better than both wavelet correlogram, and EWC in terms of all of the above evaluation measures.

5. Concluding Remarks

In this paper, a new method called GWC in CBIR was presented. GWC enhances the wavelet correlogram performance by including more directions (in addition to horizontal and vertical) to extract shape features using Gabor wavelets. Simulation results demonstrated higher performance of the proposed algorithm compared to the previous versions including wavelet correlogram and EWC in terms of average rank, precision, and recall.

6. References

[1] A. W. M. Smeulders, M. Worring, S. Santini, A. Gupta, and R.

Jain, "Content-based image retrieval at the end of early years," *IEEE Trans. Pattern Anal. Machine Intell.*, 22(12), 2000.

[2] M. J. Swain, D. H. Ballard, "Color indexing," *Int. J. Comp. Vision*, 7:11-32, 1991.

[3] C. Carson, M. Thomas, S. Blongie, J.M. Hellerstine, and J. Malik, "Blobworld: a system for Region-Based Image Indexing and Retrieval," *Proc. SPIE Visual Information Sys.*, pp. 509-516, 1999.

[4] G. Pass, R. Zabih, J. Miller, "Comparing images using color coherence vectors," *Proc. of 4th ACM Multimedia Conf.*, 1996.

[5] M. K. Mandal, S. Panchanathan, and T. Aboulnasr, "Fast wavelet histogram techniques for image indexing," *J. Comp. Vision and Image Understanding*, 75(1/2):99-110, 1999.

[6] J. Huang, S. R. Kumar, M. Mitra, W. J. Zhu, R. Zabih, "Image indexing using color correlograms," *IEEE Conf. Comp. Vision and Pattern Recognition*, pp. 762-768, 1997.

[7] J. Li., J. Z. Wang, G. Wiederhold, "SIMPLicity: semantics-sensitive integrated matching for picture libraries," *IEEE Trans. Pattern Anal. Machine Intell.*, 23(9):947-963, Sep. 2001.

[8] H. Abrishami Moghaddam, T. Taghizadeh Khajoei, A.H. Rouhi, "A new algorithm for image indexing and retrieval using wavelet correlogram," *Proc. IEEE Int'l Conf. Image Proc.*, 2:497-500, 2003.

[9] H. Abrishami Moghaddam, T. Taghizadeh Khajoei, A. H. Rouhi, M. Saadatmand-T., "Wavelet correlogram: a new approach for image indexing and retrieval," *Pattern Recognition*, 38(12):2506-2518, 2005.

[10] M. Saadatmand-Tarzjan, H. Abrishami Moghaddam, "Enhanced wavelet correlogram methods for image indexing and retrieval," *IEEE Conf. Image Processing (ICIP '06)*, 2005.

[11] M. Saadatmand-Tarzjan, H. Abrishami Moghaddam, "A novel evolutionary approach for optimizing content-based image indexing algorithms," Submitted to *IEEE Trans. Sys., Man, Cybernet.: Part B*.

[12] T.S. Lee, "Image representation using 2D Gabor wavelets," *IEEE Trans. Pattern Anal. Machine Intell.*, 16(10), Oct. 1996.

[13] B. S. Manjunath, W.Y. Ma, "Texture features for browsing and retrieval of image data," *IEEE Trans. Pattern Anal. Machine Intell.*, 18:837-842, 1996.

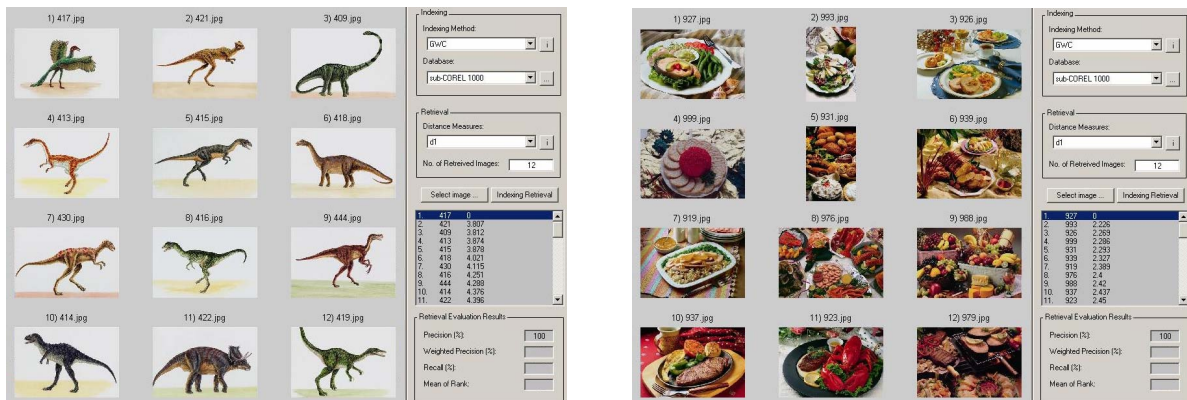


Figure 6. Results obtained for query images (a) 417 (left) and (b) 927 (right) using GWC.